Coherent Dynamic Structure Factor of Liquid Lithium by Inelastic X-Ray Scattering

H. Sinn,[1] F. Sette,[2] U. Bergmann,[2] Ch. Halcoussis,[2] M. Krisch,[2] R. Verbeni,[2] and E. Burkel[1]

[1]*Universität Rostock, D-18051 Rostock, Germany*

[2]*European Synchrotron Radiation Facility, F-38043 Grenoble, France*

(Received 5 December 1996)

We present high resolution inelastic x-ray scattering measurements of the coherent dynamic structure factor $S(Q, \omega)$ of liquid lithium at momentum transfers $0.36 \leq Q \leq 5$ Å^{-1}. The determined $S(Q, \omega)$ agrees much better with molecular dynamic simulations using the neutral pseudo-atom potential rather than the empty core potential. We observe a positive dispersion in the sound velocity confirming that in liquid lithium the longitudinal dynamics reaches a solid-like response at high frequencies. [S0031-9007(97)02529-5]

PACS numbers: 61.25.Mv, 61.10.Eq, 61.20.Ne

Recently, Canales *et al.* [1] calculated the dynamic structure factor of liquid lithium by means of molecular dynamic (MD) simulations using two different pair potentials: the empty core potential derived by Ashcroft [2] and an *ab initio* calculation for a pair potential deduced from the neutral pseudoatom method (NPA potential) [3]. Although the shapes of these two potentials are quite different, most of the calculated structural and thermodynamic properties are very similar [1]. Significant differences are observed in the calculations of the coherent part of the dynamic structure factor.

Inelastic neutron experiments on the dynamic structure factor of liquid ^{7}Li were performed by de Jong *et al.* [4]. However, these measurements yielded no decision which of the two pair potential approaches is the more favorable. The reason is that an essential part of the coherent structure factor—the Brillouin modes—could not be observed at small momentum transfers Q. Because of the momentum-energy relation for a classical particle there exists a maximum energy transfer ω at a momentum transfer Q, which is determined by the flight velocity of the incident neutron. In the neutron experiment mentioned above the Brillouin excitations were not detectable for $Q < 1.2$ Å^{-1}. Moreover, the high fraction of incoherent scattering at small Q and the uncertainties in the incoherent cross section of ^{7}Li makes it difficult to extract the coherent part from the experimental data.

In contrast, these limitations do not appear in an inelastic x-ray scattering experiment with sufficient high energy resolution. At energy transfers of about a few meV the observed intensity originates dominantly from coherent scattering. The energy-momentum relation of the photon allows an almost unlimited energy transfer at any accessible momentum transfer [5,6].

Previous experiments on liquid lithium were performed at the synchrotron laboratory HASYLAB in Hamburg [7,8]. The experiments reported here were carried out during the commissioning phase of the inelastic x-ray scattering beamline (ID16) at the European Synchrotron Facility (ESRF) in Grenoble. The x-ray radiation, coming from an undulator, was monochromized by a combination of a cryogenically cooled heat load monochromator and a silicon backscattering monochromator [Si(7,7,7) with $E = 13.8$ keV]. The analyzer, a two dimensional focusing array of silicon crystals, is positioned at a 2.5 m distance from the sample in backscattering geometry. Details of the backscattering technique and the experimental setup are discussed in Refs. [5,6]. A variation of the energy transfer was achieved by a thermal variation of the lattice parameter of the monochromator crystal. We obtained a calibration of energy shifts related to temperature differences between the two crystals by measuring a phonon dispersion curve in crystalline silicon and comparing it to results from an inelastic neutron scattering experiment [9].

The energy resolution of the spectrometer is mainly determined by the intrinsic reflection width of the silicon crystals, the alignment, and the focusing performance of the analyzer. The resolution function $R(\omega)$ was measured at the structure factor maximum of polymethylmethacrylate (PMMA), yielding an energy resolution of 11 meV (FWHM).

As a sample we used pure lithium at a temperature of 215 °C, well above the melting point ($T_M = 180.5$ °C). In order to avoid a contamination of the sample, it was contained in a UHV chamber with beryllium windows, highly transparent for the x-ray beam.

The inelastic x-ray scattering cross section with energy transfer ω and momentum transfer Q, following the analysis of Chihara [10], can be written in a liquid metal as

$$\frac{d\sigma}{d\Omega\, d\omega}(Q, \omega) \propto \sigma_T \{[\, f_i(Q) + \rho_v(Q)]^2 e^{\frac{1}{2}\hbar\omega\beta} S(Q, \omega) + z S_v^0(Q, \omega) + (Z - z) S_i^{\mathrm{inc}}(Q, \omega)\}, \quad (1)$$

where σ_T is the Thomson cross section, $f_i(Q)$ and $\rho_v(Q)$ are the form factors for the ions and for the valence electrons, Z is the number of electrons, and z is the number of the valence electrons.

$S(Q,\omega)$ is equal to the coherent dynamic structure factor appearing in the cross section for neutron scattering. The exponential factor in Eq. (1) (detailed balance factor) is a first order quantum correction that allows one to consider $S(Q,\omega)$ as a symmetrical function in ω [11].

The incoherent dynamic structure factor for the valence electrons, $S_v^0(Q,\omega)$, arises from excitations of the electron gas. For simple metals, $S_v^0(Q,\omega)$ can be replaced, as a first approximation, by the dynamic structure factor of a jellium $S_v^{\text{jell}}(Q,\omega)$ [10]. In this approximation, no significant incoherent scattering for energy transfers below a few eV is expected. Possible deviations from this behavior are discussed in Ref. [12].

Incoherent scattering consisting of electron-hole excitations of the core electrons is described by $S_i^{\text{inc}}(Q,\omega)$. At high Q the incoherent scattering terms $zS_v^0(Q,\omega) + (Z - z)S_i^{\text{inc}}(Q,\omega)$ turn into the Compton cross section.

The measured inelastic x-ray scattering spectra $I(Q,\omega)$ are shown in Fig. 1 for selected values of momentum transfers. The solid lines are the fits discussed in the following, and the full curve shown at the bottom of the figure is the resolution function. The spectrum is characterized by a central peak component due to quasi-elastic scattering, and the two side components are due to inelastic x-ray scattering (energy loss and gain) from collective atom excitations, generally referred to as Brillouin lines. At low Q values, the dispersion of these lines, and therefore the persistence of a propagating collective behavior of this excitations, is evident already in the raw data.

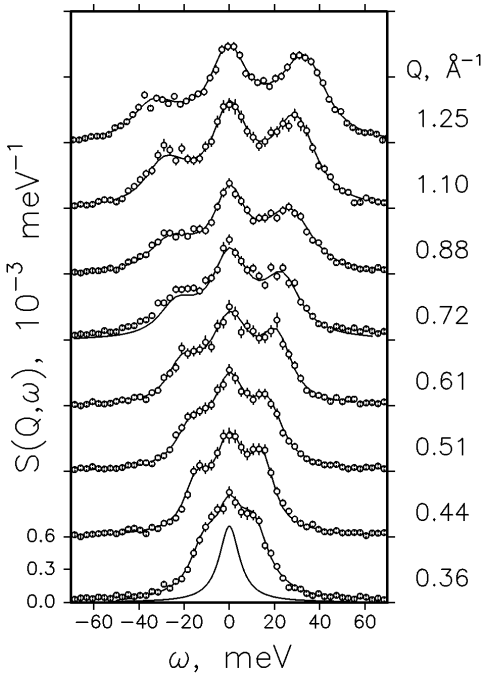

FIG. 1. Experimental data for liquid lithium from inelastic x-ray scattering. The full lines denote fits according to the model of the extended hydrodynamic modes, the full curve at the bottom is the resolution function of the spectrometer.

The first steps of the data reduction were the normalization to a monitor signal and the subtraction of the empty cell measurements. In order to get our results comparable to the available results from neutron scattering, we analyzed the coherent structure factor $S(Q,\omega)$ in terms of the model of the extended hydrodynamic modes [13]:

$$S(Q,\omega) = \frac{A_0}{\pi}\frac{z_0}{\omega^2 + z_0^2} + \frac{A_s}{\pi}\frac{z_s + (\omega + \omega_s)\tan\phi}{(\omega + \omega_s)^2 + z_s^2} + \frac{A_s}{\pi}\frac{z_s - (\omega - \omega_s)\tan\phi}{(\omega - \omega_s)^2 + z_s^2}. \quad (2)$$

Equation (2) describes a central Lorentzian (Rayleigh line) and two asymmetrical Lorentzians (Brillouin lines) at $\pm\omega_s$, where ϕ determines the asymmetry. The parameters A_i and z_i define the areas and the half-widths of the three lines. The measured intensity can be described by a convolution of the dynamic structure factor and the resolution function

$$I(Q,\omega) \propto \int_{-\infty}^{\infty} e^{\frac{1}{2}\hbar\omega'\beta} S(Q,\omega') R(\omega - \omega')\, d\omega'. \quad (3)$$

Using all six parameters in Eq. (2) as adjustable, the χ^2 values of the fitting functions were in the expected range of statistical noise of the data.

The results for the deconvoluted fitting curves at three different Q values are shown in Fig. 2 as vertical bars. The half lengths of the bars correspond to the 1σ uncertainty of the fitting curves due to the statistical error in the raw data. An intensity normalization of the x-ray data in Fig. 2 was achieved by setting the second frequency moment of $S(Q,\omega)$ to the theoretical value

$$\frac{Q^2}{M\beta} = \int_{-\omega_l}^{\omega_l} \omega^2 S(Q,\omega)\, d\omega, \quad (4)$$

where M is the particle mass and ω_l is a suitable integration limit [14].

The full lines and the dashed lines are molecular dynamic calculations performed by Canales *et al.* using the NPA potential and empty-core potential, respectively. Clearly, the NPA simulation fits much better the experimental data at $Q = 0.72$ Å^{-1} and $Q = 1.25$ Å^{-1}. At higher Q values the dependence of dynamic structure factor on differences in the pair potential is much weaker. The MD curves and the measured spectra at $Q = 3.53$ Å^{-1} are indistinguishable within the experimental error.

The dispersion $\omega_s(Q)$ of the Brillouin lines in comparison with results from MD simulation and inelastic neutron scattering is shown in Fig. 3. The results from the NPA simulation (solid line) are in good agreement with the dispersion from inelastic x-ray scattering, with respect to the maximum observed frequency. This implies that the

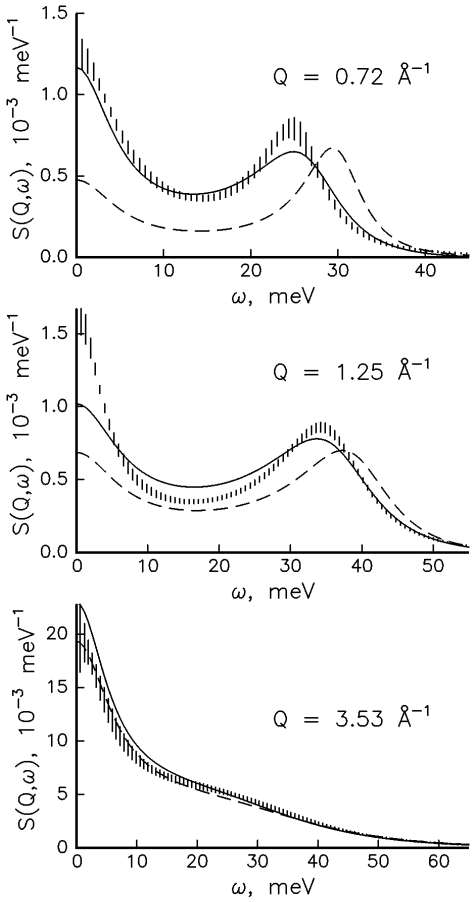

FIG. 2. Deconvoluted fitting curves for $Q = 0.72$, 1.25, and 3.53 Å^{-1}. The vertical bars represent the error interval due to the statistical uncertainty of the data. The full line is a result from molecular dynamics [1] with the NPA potential; the broken line corresponds to simulations with the empty core potential.

NPA method of calculating the pair potential leads to a better description of the repulsive part of the potential and, consequently, gives a more realistic description of the generalized Einstein frequency as described, e.g., in Ref. [15]. The dispersion of the data from the MD simulation with the empty-core potential (dashed line) lies significantly above the x-ray data in the small Q range.

The discrepancy between x-ray data and the neutron data for $Q > 1.2$ Å^{-1}, which suggest a lower lying dispersion, is not fully understood now. However, for a further investigation, the error bars of the neutron data have to be diminished.

For small Q values, the dispersion observed by inelastic x-ray scattering is steeper than the slope corresponding to the macroscopic sound velocity in the liquid (dashed-dotted line in Fig. 3). This so-called positive dispersion was observed before, e.g., on liquid cesium by inelastic neutron scattering [16] and to a much larger extent in water [6]. For a monoatomic liquid this effect is associated with the onset of a viscoelastic shear relaxation (dotted line) [17].

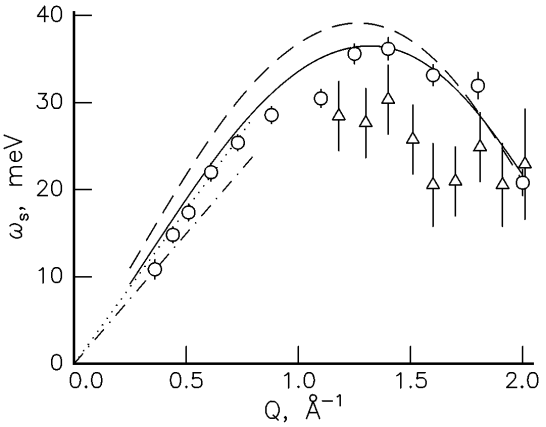

FIG. 3. Dispersion relation of the Brillouin mode. Open circles: this work; open triangles: inelastic neutron scattering [4]; solid line: MD simulations [1] with the NPA potential; dashed line: empty core potential; dot-dashed line: macroscopic sound velocity; dotted line: viscoelastic sound velocity [17].

In conclusion, the dispersion and the shapes of the Brillouin lines in liquid lithium could be obtained from high resolution inelastic x-ray scattering. The high statistical accuracy of the data and the large accessible Q-ω range yields a picture of the propagating modes that is much more precise than from previous neutron scattering experiments. From the comparison with two MD simulations a preference for the NPA pair potential rather than for the empty core potential can be concluded.

We wish to thank the ESRF for the technical support and the good collaboration. This work was partially supported by the European network (ERBCHRXCT930118) and the Bundesministerium für Forschung und Technologie (05-650 WEA1). One of us (H. S.) would like to thank M. Canales for providing the data from molecular dynamics, and the participants of the EEC science program (SC1-CT91-0754), especially P. Verkerk, for fruitful discussions.

[1] M. Canales, L. E. Gonzales, and J. A. Padro, Phys. Rev. E **50**, 3656 (1994).
[2] N. W. Ashcroft, Phys. Lett. **23**, 48 (1966).
[3] L. E. Gonzales, D. J. Gonzales, M. Silbert, and J. A. Alonso, J. Phys. Condens. Matter **5**, 4283 (1993).
[4] P. H. K. de Jong, P. Verkerk, and L. A. de Graaf, J. Non-Cryst. Solids **156–158**, 48 (1993).
[5] E. Burkel, *Inelastic Scattering of X-Rays with Very High Energy Resolution* (Springer, Berlin, 1991).
[6] F. Sette, G. Ruocco, M. Krisch, U. Bergmann, C. Masciovecchio, V. Mazzacurati, G. Signorelli, and R. Verbeni, Phys. Rev. Lett. **75**, 850 (1995).
[7] E. Burkel and H. Sinn, J. Phys. Condens. Matter **6**, A225–A228 (1994).
[8] E. Burkel and H. Sinn, Int. J. Thermophys. **16**, 1135–1142 (1995).

[9] J. Kulda, D. Strauch, P. Pavone, and Y. Ishii, Phys. Rev. B **50**, 13 347 (1994).
[10] J. Chihara, J. Phys. F **17**, 295 (1987).
[11] P. Schofield, Phys. Rev. Lett. **4**, 239 (1960).
[12] H. Sinn and E. Burkel, J. Phys. Condens. Matter **8**, 9369 (1996).
[13] I. M. de Schepper, P. Verkerk, A. A. van Well, and L. A. de Graaf, Phys. Rev. Lett. **50**, 974 (1983).
[14] H. Sinn, Ph.D. thesis, Universität Erlangen-Nürnberg, 1995.
[15] U. Balucani, G. Ruocco, A. Torcini, and R. Vallauri, Phys. Rev. E **47**, 1677 (1993).
[16] T. Bodensteiner, C. Morkel, P. Müller, and W. Gläser, J. Non-Cryst. Solids **117/118**, 116–119 (1990).
[17] J. B. Boon and S. Yip, *Molecular Hydrodynamics* (McGraw-Hill, New York, 1980).